Colloid Polym 277:1117–1124 (1999)

ORIGINAL CONTRIBUTION

Y. Yamaguchi
Y. Inaba
H. Uchiyama
H. Kunieda

Anomalous phase behavior of water-soluble polyelectrolyte and oppositely charged surfactants

Received: 9 February 1999
Accepted in revised form: 23 June 1999

Y. Yamaguchi · Y. Inaba
H. Kunieda (✉)
Graduate School of Engineering,
Yokohama National University,
Tokiwadai 79-5, Hodogaya-ku,
Yokohama 240-8501, Japan
e-mail: kunieda@ynu.ac.jp
Fax: +81-45-3394190

H. Uchiyama
Department
Proctor & Gamble Far East Inc.
17 Koyo-cho Naka 1-chome
Higashinada-ku, Kobe 658, Japan

Abstract Aqueous mixtures of anionic surfactants with cationically substituted quaternary ammonium derivatives of hydroxyethylcellulose, JR and LR series, were investigated by several techniques. On adding sodium dodecyl sulfate (SDS) to a polyelectrolyte solution, phase separation with precipitation occurs in a co-operative way, and redissolution of precipitation is observed at the critical micelle concentration (CMC) of SDS. This is due to admicelle formation on the polyelectrolyte. The phase separation for the two-headed anionic surfactant systems is also seen, while the concentration where this takes place is near the CMC of the surfactant. This is remarkable in the case of the triethanolamine cocoyl glutamate (TCG)–JR 400 system, in which TCG has a CMC over 1 order of magnitude smaller CMC than that of SDS. Surface tension and the dynamic light scattering measurements show the existence of not only electrostatic interaction between the cationic polyelectrolyte and the two-headed anionic surfactant but also intraction between the adsorbed polymers. The scaling analysis of the precipitation line of the surfactant with polyelectrolyte concentration elucidates that one molecule of TCG can neutralize approximately two charges on JR 400.

Key words Adsorption manner · Phase separation · Resolubilization · Electrostatic interaction and intraction · Scaling law

Introduction

For the behavior of colloidal particles in solution, the surface charge is an important factor for many applications. The sign and the magnitude of the surface charge are directly related to colloid stability and they profoundly influence the adsorption characteristics of the particles.

Water-soluble cellulose derivatives are large-scale commercial products which are used in many industrial applications. Since these are highly biodegradable, their use has recently become quite significant due to concerns about environmental pollution. Of particular interest in this investigation are cationically modified quaternary ammonium derivatives of hydroxyethylcellulose (HEC). HEC is a water-soluble compound, and because of its compatibility it is used as a thickener, a protective colloid, or a water-retarding agent in cosmetic products, lubricant materials for hair in personal care products, and in many other industrial applications. Quaternary ammonium derivatives of HEC, which for commercial products are known as the polyquaternum-10 series, are available with viscosities ranging from 75 to 12,000 cP. The chemical modification of the degree of substitution drastically causes a change in the macroscopic properties [1–3]. Tanaka et al. [4, 5] have shown that unmodified HEC is present as individual molecules which interact through hydrodynamic forces, while the modified systems form transient networks in solution.

The macroscopic properties of such systems can be further improved and optimized by the addition of surfactants. Combinations of polyquaternum-10 solu-

tions have been investigated by Goddard and coworkers [6–8]. It was concluded from these studies that the anionic surfactants bind to the cationic charges of the polymer, and the tails of the surfactant act as cross-links between the different polymers.

In this study, a noticeable wider two-phase region was observed when an anionic surfactant with two hydrophilic parts is used instead of a single-headed surfactant. The purpose of this work is to establish the phase separation mechanism induced between cationically modified HEC and various anionic surfactants. Since the linear phase boundaries strongly hint at the adsorption manner of the surfactant on the polymer, the analysis was carried out by means of a power law. Interestingly, the presence of a cationic surfactant in the polymer–anionic surfactant system is also effective. Moreover, the use of the double-chain anionic surfactant shows the extended two-phase region as well as that of the double-headed surfactant. Both cases were also investigated by means of phase diagrams.

Experimental

Materials

Quaternary ammonium derivatives of HEC (polyquaternum-10) were produced by Amerchol. The JR series polymers JR125, JR400, and JR30M are highly cationically substituted and the viscosities of their aqueous solutions are in the order JR125 < JR400 < JR30M. These polymers have a cellulose backbone derived from natural, renewable resources. They are reacted with a trimethyl ammonium substituted epoxide. The LR series polymers have lower degree of cationic substitution than the JR series. A typical molecular structure of a polymer is shown in Fig. 1. These polymers were used without further purification.

The following surfactants were also employed without further purification: sodium dodecyl sulfate (SDS), $C_{12}H_{25}SO_4Na$, (Sigma Chemical Co); dodecyl trimethylammonium bromide, $C_{12}H_{25}N(CH_3)_3Br$, (Tokyo Kasei Industry Co., Tokyo); ammonium lauryl sulfate, $C_{12}H_{25}SO_4NH_4$, (Tayca Co., Osaka); ammonium trioxyethylene dodecyl sulfate AE_3S as a 25% aqueous solution (Tayca); triethanol amine cocoyl (mixture of acyl chain $C_{12}CO{\sim}C_{18}CO$) glutamate (TCG) as a 29.9% aqueous solution which has a pH of 5.24 (Ajinomoto Co.); sodium bis (2-ethylhexyl) sulfosuccinate (Aerosol OT) (Sigma-Aldrich Chemie, Steinheim, Germany).

Methods

All polymer solutions whether in the presence or absence of surfactants were continuously stirred for at least 30 min and were kept in a water bath for several days at 25 °C. Measurements was carried out assuming that all samples reached the equilibrium state. The appropriate amount of surfactant was added to a glass tube containing the polyelectrolyte powder. The phase diagrams of HEC–anionic surfactant aqueous solutions were prepared by visual observation at 25 °C.

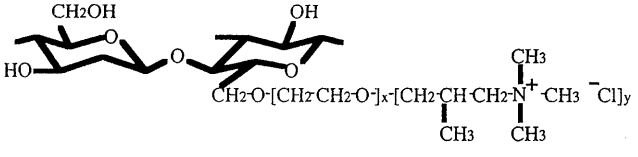

Fig. 1 Schematic molecular structure of polyquaternum-10. A portion (Y) of $(CH_2CH_2O)_x$ is substituted by the cationic function

Surface tension measurements were performed with an automatic surface tensiometer (Kyowa Kaimen Kagaku Co.), based on the Wilhelmy plate method. The solutions were thermostated and measurements were continued until the surface tension value leveled off. Samples in which precipitation occurred were decanted, and the supernatant solutions were utilized for the measurements.

Dynamic light scattering (DLS) measurements were carried out to determine and confirm the presence and the size of the aggregates. The solutions were not filtered through the pore-size micromembrane in order to prevent distortion of the real structures. DLS measurements were made using an Otsuka Denshi photomultiplier with a He/Ne laser (632.8 nm) and an advanced digital correlator. An inverse Laplace transformation was performed on the autocorrelation curve data to obtain the distribution of relaxation times. With the scattering vector Q, the equation

$$\tau = \left(Q^2 D_{\text{eff}}\right)^{-1} , \tag{1}$$

and the Stokes–Einstein equation

$$D_0 = \frac{kT}{6\pi\eta_0 R_{\text{H}}} \tag{2}$$

an effective hydrodynamic radius, R_{eff}, can be calculated, containing the structure factor $S(Q)$:

$$D_{\text{eff}} = \frac{D_0}{S(Q)} \tag{3}$$

All solutions were thermostated at 25 °C.

Differential scanning calorimetry (DSC) measurements were carried out on the powdered polymer and even aqueous solutions of it showed an endothermic peak on heating. Measurements were made with a Rigaku Thermo plus Micro DSC in a temperature range from 0 to 100 °C and with a scanning rate of 2.0 °C/min.

Results and discussion

The experimental results have to be discussed while keeping in mind that they were obtained on commercially produced materials. These materials are not pure compounds. For this reason we cannot expect to observe the behavior which is typical for well-defined surfactants, where in general a sharp critical micelle concentration (CMC) and/or clear breaks from the monomer to micellar state are present in surface tension measurements.

Phase diagram and phase behavior

Phase separation with precipitation is observed when the anionic surfactant is added to the polyelectrolyte solutions. With increasing anionic surfactant concentration, the amount of precipitation gradually decreases, and finally resolubilization of precipitation takes place. Such phase behavior is seen for all polymers but the phase boundaries are likely to be dependent on the molecular weight and the cationic charge density.

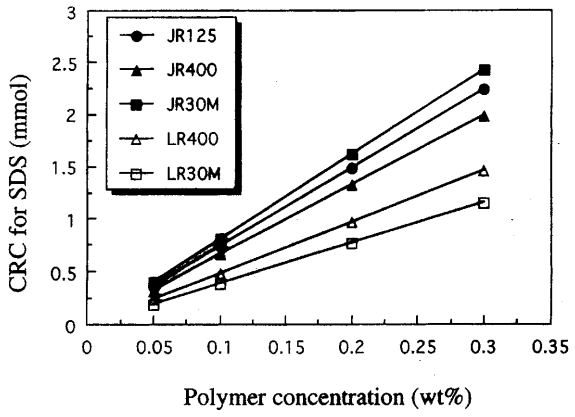

Fig. 2 Effect of critical resolubilization concentration (*CRC*) of sodium dodecyl sulfate (*SDS*) on the resolubilization phenomena of the polymer. $T = 25$ °C

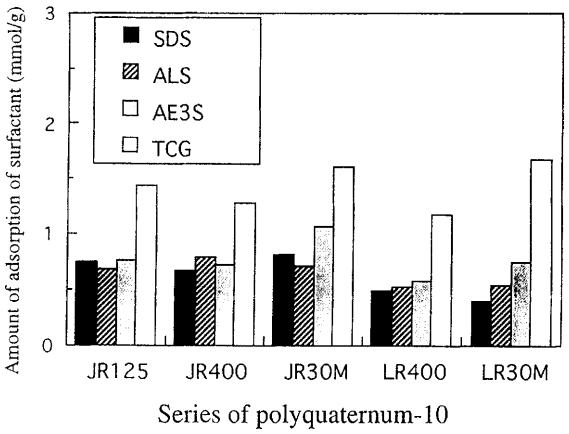

Fig. 3 Amount of anionic surfactant adsorbed on the different polymers. The amounts adsorbed were calculated from the lines for the *CRC* as shown in Fig. 2

Table 1 Amount of sodium dodecyl sulfate (*SDS*) adsorbed on each polyquaternum-10 polymer

Polymer	Amount of adsorption on polymer (mmol/g)
JR 125	0.75
JR 400	0.67
JR 30M	0.81
LR 400	0.49
LR 30M	0.39

The concentrations where the resolubilization, which corresponds to the critical resolubilization concentration (CRC), occurs are rather characteristic. The phase diagrams for the CRC of SDS on the various polyelectrolyte species are shown in Fig. 2. The results for all the polymer systems imply a proportional increase in the CRC within the polyelectrolyte concentration range 0.05–0.3 wt%. It is noticeable that each slope of the lines corresponds exactly to the amount of SDS adsorbed per gram of polyelectrolyte. Since SDS is the most typical 1-1 type anionic surfactant, the estimation results of each line in Fig. 2 probably allow the cationic charge density of each polyelectrolyte to be determined. The amounts of SDS adsorbed on each polyelectrolyte are listed in Table 1. In fact the polymerization numbers of CH_2CH_2O, X, and of $CH_2CH(CH_3)CH_2N^+(CH_3)_3Cl^-$, Y, are not clear; however it can be seen from Table 1 at least that the JR series polymers have a charge density approximately twice as high as that of the LR series.

To compare the adsorption behavior of each surfactant, the amounts of surfactant adsorbed on the different polymers were estimated from the slopes, such as in Fig. 2. The experiments for the determination of the CRC were carried out in the concentration range of each polymer from 0.05–0.3 wt%. It can be seen in Fig. 3 that the adsorption force of TCG on the polymer is dominant over that of the other polyelectrolytes. Remarkably this occurs for the JR 30M series polymers, which have the highest molecular weight. It is conceivable that the hydrophobic part of the polyelectrolyte strongly affects the attainment of the peptization of precipitation. The effect of the kind of counterions and thus, the dissociation degree and the size, is much smaller.

To know why a large amount of TCG binds on the polymer compared to the other surfactants, we focus especially on the JR 400–surfactant systems. Samples of JR 400 are easy to prepare due to the middle property on the viscosity. Since the concentration can generally induce a conformational transition of polymer molecules, it is noteworthy that the conformational change of JR 400 must be significant for the resolubilization behavior [9–11]. The phase diagrams of SDS AE_3S and TCG–JR 400 ternary systems wide concentration range of JR 400 are shown in Fig. 4. In the case of TCG (Fig. 4c), the two-phase region is fairly extended in comparison to the other surfactants: this is due to the different resolubilization behavior. The linear increase for SDS with JR 400 concentration is observed in the wide concentration range of JR 400, while the lines for AE_3S and TCG are subdivided by at least three different JR 400 concentration regions. This probably means that the adsorption mechanism of two-headed amphiphiles is related to the polyelectrolyte performance with concentration [9–11].

The slopes of the plots in Fig. 4 correspond approximately to the scaling law that is characteristic for the polyelectrolyte–surfactant system. In Table 2 the calculated exponents are listed and the experimental data nicely fit the power law, which is based on the following equation [12];

$$c_S = \beta c_P^{\alpha} \tag{4}$$

where c_S is the surfactant concentration, c_P the JR 400 concentration, α the exponent, and β a constant.

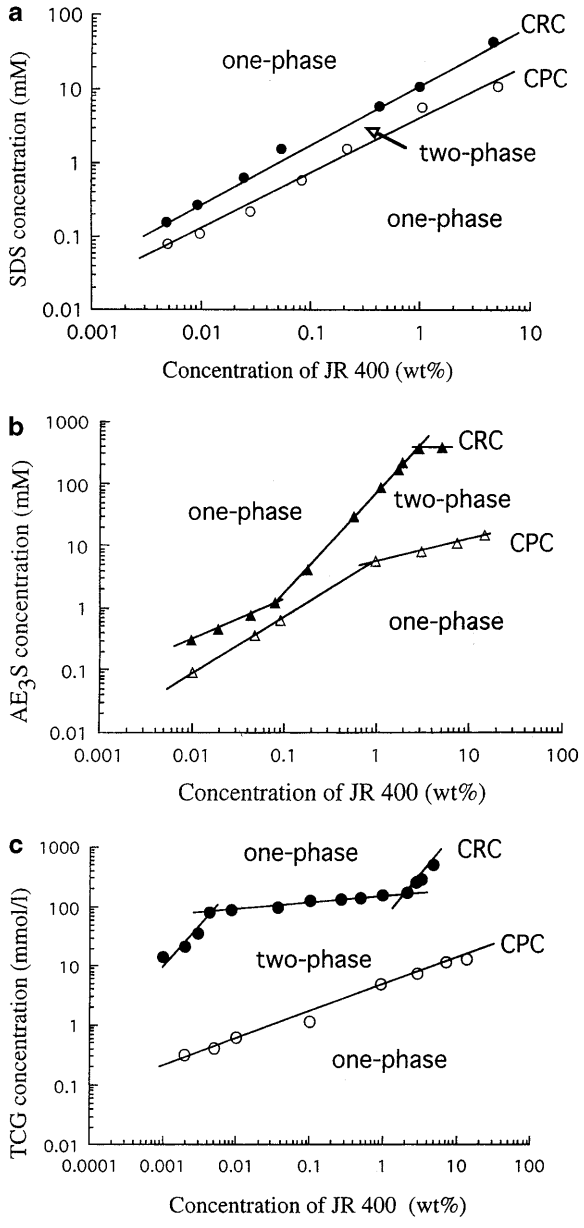

Fig. 4a–c Phase diagrams of anionic surfactant–*JR 400* ternary systems showing the *CRC* and the critical precipitation concentration (*CPC*). $T = 25$ °C. **a** *SDS* **b** ammonium trioxyethylene dodecyl sulfate (AE_3S) **c** triethanol amine cocoyl glutamate (*TCG*)

The lines for the critical precipitation concentration (CPC) can almost be indicated by only one scaling parameter for all systems. The differences in the anionic surfactants slightly influence the start of the phase separation. This can be explained if precipitation is mainly induced by the electrostatic interaction between the cationic charges on JR 400 and the anionic surfactant; therefore, the interaction between the polymers can be neglected. It is pointed out here that the magnitude of α for the CPC is related to a cooperative mechanism for precipitation; hence, the result that 0.44 for TCG is approximately half of the 0.76 for SDS suggests the binding of two charges of JR 400 per TCG molecule.

Table 2 Scaling parameter for *JR 400*–anionic surfactant ternary systems. Each parameter was estimated from the results in Fig. 5

Surfactant	α for critical precipitation concentration	α for critical resolubilization concentration
SDS	0.76	0.80
Ammonium trioxy ethylene dodecyl sulfate	0.71	0.65, 1.61, 0.12
Triethanol amine cocoyl glutamate	0.44	5.00, 0.12, 1.32

Since the deviation from JR 400 concentration is observed not only for the TCG systems but also for AE_3S systems, this anomalous phase behavior seems to be based on the two-headed structure of the surfactant. The subdivided three regimes indicate first that the adsorption manner of the surfactant depends on the JR 400 concentration. Generally, with increasing polymer concentration the polymer molecules shrink, and the interaction between the polymers is also strengthened [13]. Finally, a network structure with a high viscosity is formed in the whole space. The different scaling parameters given in Table 2 suggest that the two-headed structure of the surfactant induces a further shrinkage of the polymer. Particularly, the quite small α (0.12) in the medium polymer concentration region of the TCG system shows that intraction within the polymer and strong interaction between the polyelectrolytes are present simultaneously. In the dilute and the concentrated region of JR 400, the interaction between the adsorbed polyelectrolytes is not dominant over the intraction within JR 400 molecules. In the dilute region, it would be difficult for the polyelectrolytes to approach each other because of the long distance between them. On the other hand, in the concentrated region JR 400 molecules would already be close-packed. The interaction between JR 400 molecules thus becomes especially noticeable in the semidilute region.

Surface tension measurements

The results of the surface tension measurements of TCG–JR 400 solutions are given in Fig. 5a for different polyelectrolyte concentrations. For different JR 400 concentrations, the results tend to be the same: with increasing TCG concentration the surface tension decreases sharply and then levels off. The slight increase at higher TCG concentrations is due to the increase in the viscosity of the solutions. TCG might form a network structure in solution because of the entangled longer rodlike micelles.

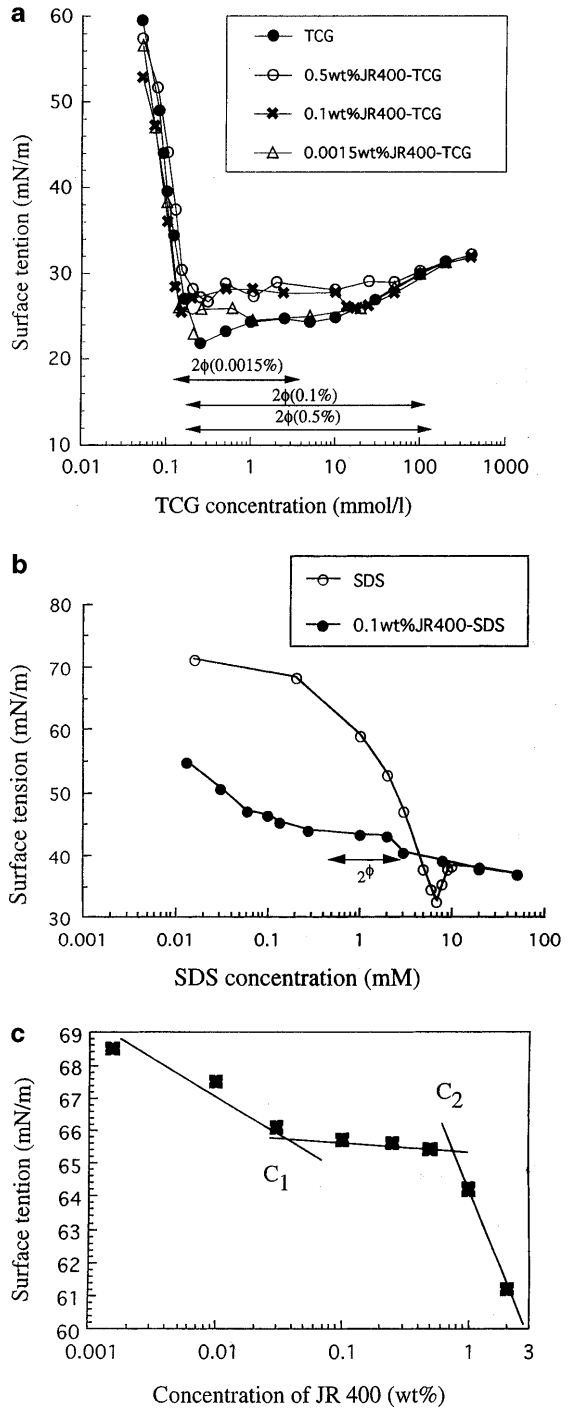

Fig. 5 **a** Surface tension values for *TCG–JR 400* aqueous solutions as a function of *TCG* concentration. Samples with precipitation were centrifuged and the supernatant solutions were utilized for the measurements. **b** Surface tension of *JR 400*–water solution **c** Change in surface tension values of *JR 400* 0.1 wt%–*SDS* solutions as a function of *SDS* concentration. All measurements were carried out at 25 °C

Assuming that the polymers adsorbed by the surfactants are hardly surface active, the quantity of surfactant can be determined by surface tension measurements [14–16]; however the results in Fig. 5a show this is not a valid assumption.

This behavior is in fact due to the surface activity of JR 400. As can be seen in Fig. 5b, JR 400 shows little surface activity in water. The two breaks observed, c_1 and c_2, are likely to be the result of the broad molecular distribution. Most surface-active material begins to aggregate in the solution at c_1, and at c_2 all the material forms micelles. This behavior has also been observed in block copolymer solutions [18].

The surface tension values of SDS–JR 400 0.1 wt% solutions are shown in Fig. 5c. The result that a smaller surface tension is detected in the dilute region of SDS, is comparable to that for the TCG system (Fig. 5a). The adsorption of SDS molecules on JR 400 forms the hydrophobic domain on the polymer. This is dominant to TCG system because one TCG molecule compensates two cationic charges of JR 400. Such behavior has also been reported in other polymer solutions with surfactants [18–20]. Systems of inorganic compounds do not have lower surface tensions than pure surfactants [21]. This contradiction is caused by JR 400 molecules with surface activity.

Dynamic light scattering measurements

In Fig. 6a we show how the diffusion coefficient of JR 400 0.1 wt%–TCG solutions change with increasing TCG concentration. The effective diffusion coefficient (D_{eff}) values were obtained by the extrapolation to zero angle where the structure factor $S(Q)$ in Eq. (3) can be ignored. In the dilute region, D_{eff} decreases with an increase in TCG concentration. With a further increase in concentration (in the resolubilization state) D_{eff} becomes much faster than in the first one-phase region, but again starts to decrease with increasing TCG concentration.

The angular dependence of the particles is shown in Fig. 6b. In the first single region, no angular dependence of D_{eff} is seen, while a gradual increase is detected in the repeptized region.

It can be deduced from the results in Fig. 6a and b that the number of bound TCG molecules increases with increasing TCG concentration but their shape seems to be almost spherical. The observed precipitation is mainly attributed to the hydrophobic effect between the tails of the TCG molecules; therefore, the magnitude of the precipitation would be quite large. To reach the resolubilization state, the aggregation might be divided to the smaller complex due to the formation of an admicelle with the head group on the solution side [22, 23]. The presence of electrostatic repulsion between

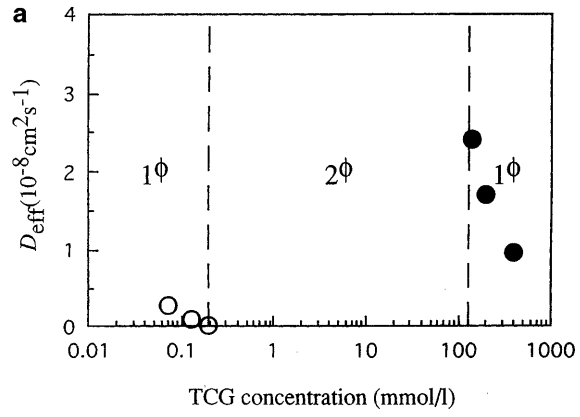

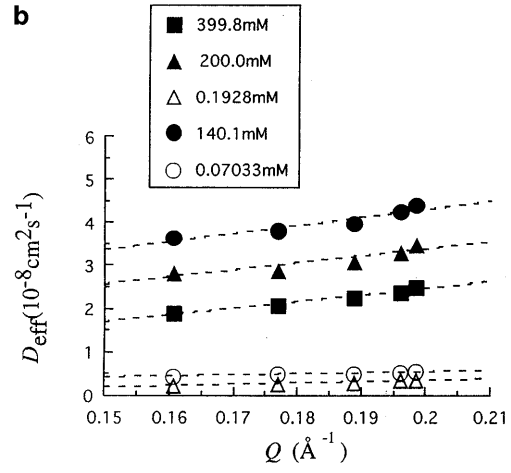

Fig. 6 **a** Effective diffusion coefficient values for *TCG–JR 400* 0.1 wt% solutions as a function of *TCG* concentration. $T = 25$ °C. **b** Angular dependence of D_{eff} at different concentrations of *TCG*. The JR 400 concentration was fixed at 0.1 wt%. $T = 25$ °C

admicelles can lead to the separation of aggregation. Consequently, a large D_{eff} is observed at the resolubilization state. With a further increase in TCG concentration, the free TCG molecules which do not contribute to the adsorption may form long rodlike micelles. The decrease in D_{eff} is thus detected in a concentrated region of TCG.

DSC measurements

DSC measurements in the presence of the anionic surfactant suggest that the total heat flow is related to the manner of adsorption. The peak is associated with the change in the hydrophobic parts from the aqueous surroundings into the lipophilic micellar state. The pure JR 400 0.1 wt% solution does not give rise to an endothermic peak with increasing scanning temperature (line a in Fig. 7). A quite small peak is observed at

Fig. 7a–c Dependence of the endothermic peak of the heating process in differential scanning calorimetry measurements as a function of temperature. **a** JR 400 1.0 wt%; **b** JR 400 1.0 wt%–AE_3S 50 mmol/l; **c** JR 400 1.0 wt%–TCG 84 mmol/l

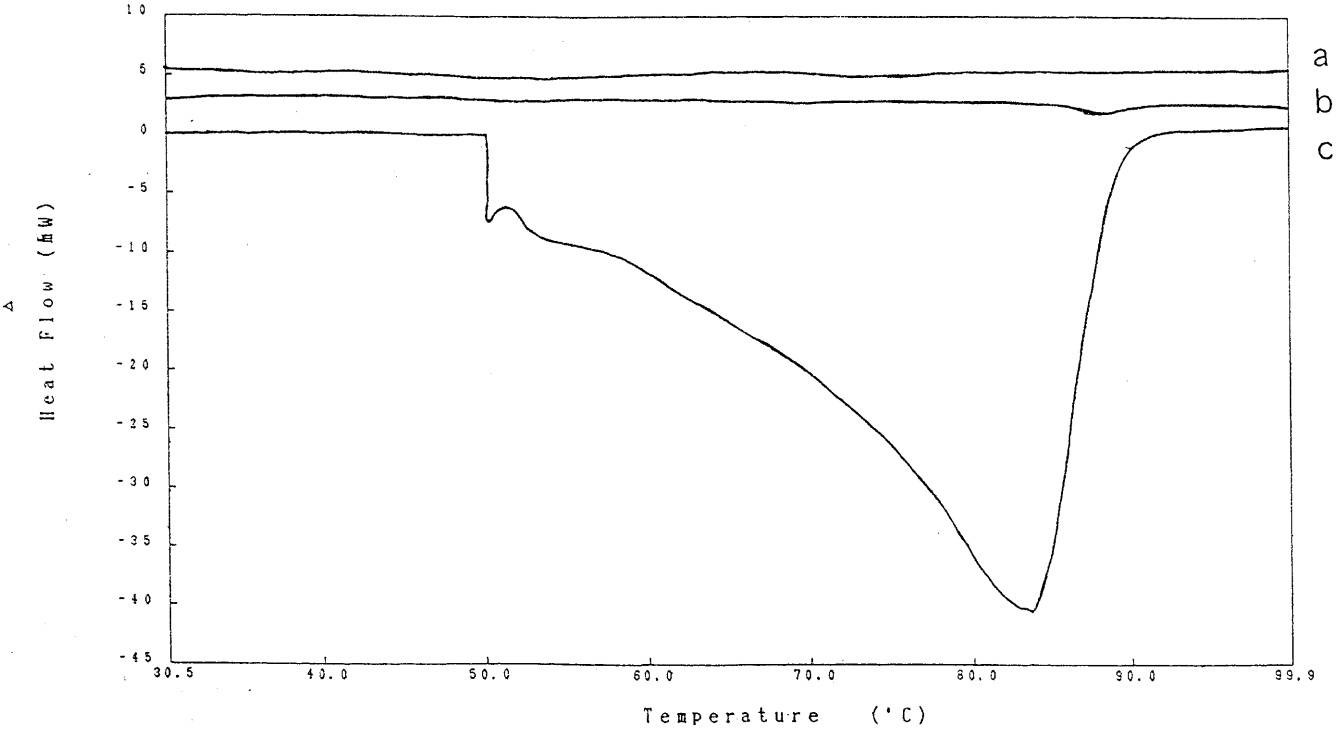

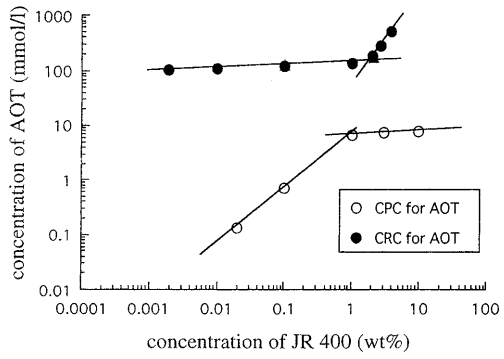

Fig. 8 Phase diagram of JR 400 aqueous solutions in the presence of Aerosol-OT (*AOT*) as a function of JR 400 concentration. $T = 25$ °C

around 90 °C for the AE_3S–JR 400 system (line b), while the TCG system (line c) shows a large endothermic peak. The observed quite large ΔH for TCG is, therefore, due to the strong compensation of the cationic charges of the polyelectrolyte and the interaction among tails on the polyelectrolytes. It can also be concluded that the strong intraction within the polymer molecule and the interaction between polymers induce the wide precipitation region.

Effect of two–tailed surfactant (Aerosol-OT)

Aerosol-OT, which is a typical two-tailed anionic surfactant, was employed instead of TCG. The phase diagram of the Aerosol-OT/JR 400/water system is shown in Fig. 8. The CRC line ($\alpha = 0.11$) is seen to be the same as for TCG (Fig. 4c). It is apparent that the two-tailed group also induces a dramatic interaction between the polyelectrolytes. Besides, even in the dilute JR 400 region, the CRC line still has the same α.

Industrially, the slight dependence of the CRC on the polymer concentration is quite important for personal care products for hair care. The fact that the dilution path of the solution by the addition of water can pass through the CRC line acts as adsorption of precipitation on hair. The dilution path can be expressed by Eq. (4) when $\beta = 1$. Whenever α for the CRC line is less than α for the dilution path, precipitation could be observed upon dilution. Hence the extended precipitation region and the nondependence of the CRC upon the polyelectrolyte concentration can enhance the possibility of adsorption on the surface of hair. As a consequence, precipitation including the polyelectrolyte acts as a lubricating mechanism between hairs during shampooing.

Conclusions

We have studied the phase behavior of cationically modified HEC–anionic surfactants in water. SDS and other anionic surfactants bind on the polymer in a co-operative way due to Coulombic forces. During adsorption, the shrinkage of the adsorbed two headed surfactant (TCG) is more remarkable. As a result, a wider phase separation takes place than for other surfactants, in particular for SDS.

With further increasing surfactant concentration, admicelles are formed on JR 400 for the SDS system. In the case of TCG, the adsorption mechanism is more complicated and depends on the JR 400 concentration. In the medium concentration region of JR 400 the molecules can approach each other, and the amount of adsorption scarcely depends on JR 400 concentration. This suggests that the intraction between tails dominates the phase behavior in the semidilute region of JR 400. Theoretically, one molecule of TCG can neutralize two cationic charges on JR 400. Since the hydrophobic force between tails of the surfactant and JR 400 is stronger than in the SDS system, the precipitation region is extended, in spite of the lower CMC of TCG compared to that of SDS.

Since the fact that the polymers shrink is quite significant for the phase separation, Aerosol-OT with two tails can attain the same amount of adsorption as two headed surfactants.

References

1. Wang KT, Iliopolos I, Andebert R (1988) Polym Bull 20:577
2. Iliopolos I, Wang K, Andebert R (1991) Langmuir 7:617
3. Biggs S, Selb J, Candon F (1992) Langmuir 8:838
4. Tanaka R, Meadaw J, Philips GO, William PA (1990) Carohydr Polym 12:443
5. Tanaka R, Meadows J, Phillips GO, Williams PA (1992) Macromolecules 25:1304
6. Goddard ED, Leung PS, Padmanabhan PA (1991) J Soc Cosmet Chem 42:19
7. Goddard ED, Leung PS (1992) Langmuir 8:1499
8. Goddard ED, Leung PS (1992) Colloids Surf 65:211
9. Hunter RJ (1991) Foundations of colloid science I. Clarendon, Oxford, p 466
10. Flory PJ (1941) J Chem Phys 9:660
11. Huggins ML (1941) J Chem Phys 9:440
12. Gennes de P-G (1979) Scaling concepts in polymer physics. Cornell University Press, Ithaca
13. Oosawa F (1971) Polyelectrolytes. Dekker, New York
14. Pashley RM, Israelachivilli JN (1981) Colloids Surf 2:169
15. Herder PJ (1990) J Colloid Interface Sci 135:346
16. Novich BE (1990) Colloids Surf 46:255
17. Hecht E, Hoffmann H (1995) Colloids Surf A 96:181

18. Lu JR, Blondel AK, Cooke DJ, Thomas RK, Penfold J (1996) Prog Colloid Polym Sci 100:311
19. Goddard ED, Hannan RB (1976) Colloid Interface Sci 55:73
20. Kästner U, Hoffmann H, Dönges R, Ehrler R (1996) Colloids Surf A 112:211
21. Yamaguchi Y, Hoffmann H (1997) Colloids Surf 121:67
22. Gaudin AM, Fuerstenau DW (1955) Trans AIME 202:958
23. Schindler PW, Fürst B, Dick R, Wolf R (1976) J Colloid Interfare Sci 55:469